A roll coating tungstate passivation treatment for hot-dip galvanized sheet steel

Cheng-Yang Tsai [a], Jen-Shou Liu [a], Pei-Li Chen [b], Chao-Sung Lin [a],*

[a] Department of Materials Science and Engineering, National Taiwan University, 1, Roosevelt Road, Section 4, Taipei 106, Taiwan
[b] New Materials R&D Department, China Steel Corporation, 1, Chung Kang Road, Hsiao Kang, Kaohsiung 802, Taiwan

ARTICLE INFO

ABSTRACT

A tungstate passivation treatment was performed on hot-dip galvanized steel via a roll coating process. The effect of anion (phosphate and nitrate) in the tungstate solution on the microstructure and corrosion resistance of the passive film was explored. The surface morphology of the GI steel slightly changed after roll coating using tungstate/phosphoric and tungstate/nitric solutions. Cross-sectional transmission electron microscope characterization revealed that the passive film prepared by the tungstate/phosphoric solution consisted of a thin compact layer, whereas that prepared by the tungstate/nitric solution was relatively thick and porous. The reduction of tungstate anion to low-valent tungsten oxide and metallic tungsten was also observed. Compared with nitrate anion, the presence of phosphate anion in the solution resulted in zinc phosphate, less metallic tungsten, and more hexavalent tungsten species in the passive film. As a result, the passive film prepared by the tungstate/phosphoric solution displayed a better corrosion resistance than that prepared by the tungstate/nitric solution, as evaluated by polarization measurement and salt spray test.

© 2011 Elsevier B.V. All rights reserved.

1. Introduction

Zinc coating on hot-dip galvanized (GI) steel provides excellent sacrificial protection over the steel substrate. To protect the GI steel against corrosion during transportation and storage, a passivation treatment is generally adopted, such as hexavalent chromium-based passivation treatment. However, a strict restriction was imposed on the use of chromate passivation because of the toxicity of hexavalent chromium. Thus, several non-chromate passivation treatments have been developed such as phosphate-based [1–7], cerium-based [8,9], molybdate-based [10–16], and tungstate-based treatments [17,18]. Unlike hexavalent chromium, tungstate is less harmful to the environment and is an effective corrosion inhibitor for zinc [19–21]. Da Silva et al. [18] investigated a tungstate/phosphoric conversion coating treatment on pure zinc and electrogalvanized steel via an immersion coating process. They found that the conversion coating showing the optimal corrosion resistance was prepared after 1 min of immersion in the solution at pH 3 containing 0.1, 0.3 or 0.5 M sodium tungstate. Furthermore, the conversion process has been shown to commence as the interfacial pH exceeded 5. The presence of WO_4^{2-} in the coating played an inhibition role in preventing the coating from corrosion. However, the corrosion protection of the tungstate conversion coating was still inferior to the chromate coating [18].

The study of passivation treatments for Zn-coated steel via an immersion coating process is abundant in the literature, whereas the passivation treatment conducted using a roll coating process is still scarce. Roll coating is a process of applying a protective coating by passing the sheet substrate through a pair of rollers. This technique is extensively used in the coil coating industry, such as the coating process for steel coil [22]. Industrial steel coil roll coating process generally employs a baking process to facilitate the formation of the coating. During baking, the concentration of the various ions in the liquid film on the steel coil increases as water evaporates. This is different from the coating formed by the immersion coating process, where the reacting species deplete in the diffusion layer over the surface during growth of the conversion coating. Further, the microstructure and the formation mechanism of the conversion coating on GI steel prepared by the roll coating process are less well studied compared with that prepared via the immersion coating process. In this study, a tungstate passivation treatment on GI steel was performed by a roll coating process, with an emphasis on the effect of phosphate and nitrate anions. The composition, microstructure, and corrosion resistance of the tungstate passive film were related to the distinct anions present in the solution. Furthermore, the growth behavior and corrosion resistance mechanism of the tungstate passive film on GI steel are proposed and discussed.

2. Experimental

2.1. Passivation treatment

The material used in this study is commercial GI steels from China Steel Co., Taiwan. Interstitial-free sheet steels were hot-dip galvanized in a molten zinc bath containing 0.2 wt.% aluminum at 460 °C. The galvanizing line speed was approximately 120 m/min. After galvanizing

---

* Corresponding author. Tel.: +886 2 33665240; fax: +886 2 23634562.
E-mail address: cslin@ntu.edu.tw (C.-S. Lin).

process, a skin pass rolling was used to improve flatness of the zinc surface. The surface roughness of the zinc surface was about 0.7 µm and the thickness of the zinc layer was around 10 µm. The GI plates (150×100×0.8 mm) were degreased in an alkaline solvent (Model PALKIN-N 364S, Nihon Parkerizing Co., Japan), cleaned and rinsed with deionized water, and finally dried in a stream of hot air. The passivation treatment was conducted by a roll coating process using a tungstate solution. The tungstate passivation solution was prepared by adding 0.08 mole sodium tungstate ($Na_2WO_4.2H_2O$) to around 1 L deionized water and the pH of the resultant solution was approximately 9.8. The solution pH was then adjusted to 2.5 with the addition of phosphoric or nitric acids so as to enhance the formation of the passive film. As a result, two tungstate solutions were studied, including tungstate/phosphoric and tungstate/nitric solutions. The roll coating process was performed by applying the passivation solution onto the GI steel by a bar coater (No. 3, wire diameter: 0.07 mm, R.D.S., Webster, New York) with a roll speed of 75 mm/s at room temperature, followed by baking in an electrical oven (Model HS-G02, Hong Seng Co., Taiwan) at 200 °C for 12 s, and then left for a final cooling at ambient temperature.

2.2. Microstructural characterization

The surface morphology of the passive film was investigated using a JEOL JXA-8200 scanning electron microscopy (SEM) and the images were recorded at backscattered electron (BSE) mode. Cross-sectional transmission electron microscope (TEM) specimen of the passive film was prepared using a focused ion beam instrument (FEI Nova-200 NanoLab Dual Beam) and examined using a FEI Tecnai F20 G2 TEM at an accelerating voltage of 200 kV. Besides, the composition of the passive film was measured via energy dispersive spectrometry (EDS) incorporated in TEM and the crystallinity was identified by the selected area electron diffraction (SAED) technique. Finally, X-ray photoelectron spectroscopy (XPS) analysis was carried out using a PHI Quantera SXM Scanning X-ray Microscope with an Al Kα monochromated source. All spectra were corrected using the signal of C 1s peak at 284.5 eV.

2.3. Corrosion resistance evaluation

The corrosion resistance of the passive film was evaluated by polarization measurement, which was conducted in aerated 5 wt.% sodium chloride (NaCl) solution using a conventional three-electrode cell system via a Model 263A Potentiostat/Galvanostat (EG&G Instruments). The working electrode was the as-received GI steel or the passivated GI steel with an exposed area of 1 cm^2. A platinum plate with an exposed area of 16 cm^2 and a commercial saturated calomel electrode (SCE) were used as the counter and reference electrodes, respectively. All polarization measurements were performed after 20 min of immersion. The polarization curves were measured by sweeping the potential in the positive direction with a scan rate of 1 mV/s. The sweep range was from an initial potential of −0.4 V to a final potential of 0.8 V relative to the open circuit potential (OCP). The polarization measurement of each sample was repeated at least three times for the as-received GI steel and five times for the passivated GI steel to ensure the reproducibility of the data.

3. Results

3.1. Surface morphology

Fig. 1 shows the surface morphology under SEM/BSE mode of the as-received GI steel, the GI steel treated with tungstate/nitric and tungstate/phosphoric solutions. The as-received GI steel displayed a typical morphology composed of plateau-like and valley-like regions (Fig. 1a), in which the plateau-like regions resulted from the contact
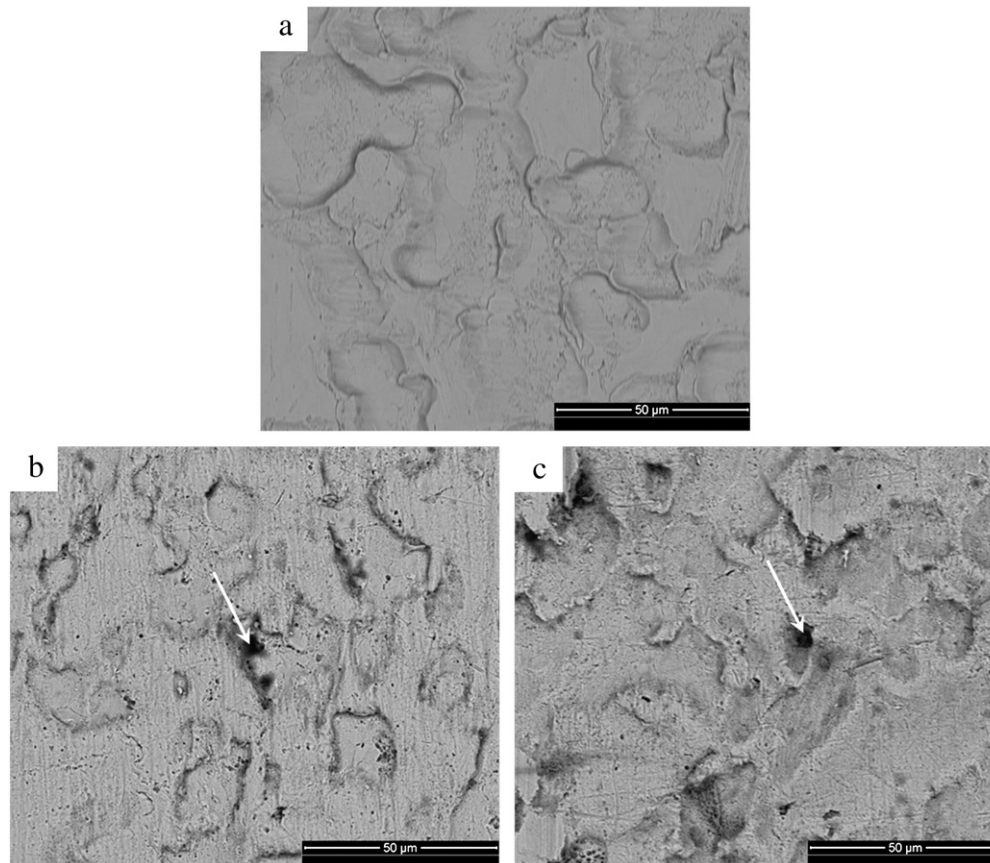

Fig. 1. Surface morphology of (a) the as-received GI steel, the GI steel treated with (b) tungstate/nitric and (c) tungstate/phosphoric solutions.

of the zinc coating with the skin pass rollers. After the tungstate passivation treatment, several dark-contrast spots (indicated by the arrow in Fig. 1b and c) were observed. Moreover, the specimens treated with tungstate/nitric and tungstate/phosphoric solutions exhibited insignificant difference in the surface morphology, specifically dark-contrast spots were randomly presented in both the micrographs of Fig. 1b and c. EDS analysis showed that more oxygen and less zinc were detected on the dark-contrast spots compared with the light-contrast areas. Therefore, the passive film associated with the dark-contrast spots was thicker than that associated with the light-contrast areas. The presence of the thicker passive film could be related to the local enhanced dissolution of the Zn substrate. This enhanced dissolution is likely owing to the defects of the native oxide layer or the impurity on the hot-dip Zn coating.

3.2. Cross-sectional TEM characterization

Fig. 2a shows a cross-sectional TEM micrograph of the passive film prepared by the tungstate/nitric solution. The film was about 100 nm in thickness and contained spherical voids frequently observed in the midst of the film (indicated by the arrow in Fig. 2a). Wen et al. [23] reported a similar structure for the trivalent chromium conversion

Table 1
TEM/EDS results of the distinct regions (marked by 1, 2, and 3 in Fig. 2a) of the passive film prepared by the tungstate/nitric solution.

Distinct regions	Atomic percentage			
	Zn	O	W	N
1	63	33	3	1
2	24	65	7	4
3	12	70	12	6

coating on electrogalvanized steel, in which large voids were found to reside mainly at the center of the passive film formed after 30 min of baking at 90 °C. EDS analyses at the region marked by 1, 2, and 3, respectively, in Fig. 2a are listed in Table 1. It can be seen in Table 1 that the zinc content increased and the oxygen, tungsten, as well as nitrogen content decreased along the depth of the passive film. The passive film prepared by the tungstate/phosphoric solution was more compact than that prepared by the tungstate/nitric solution, as shown by comparing Fig. 2a to b. The thickness of the tungstate/phosphoric passive film ranged from 30 to 60 nm. EDS analysis revealed that the passive film was composed of Zn (23 at.%), O (67 at.%) and traces of P (8 at.%) and W (2 at.%) species. The SAED patterns inset in Fig. 2a and b revealed that both the passive films had poor crystallinity.

3.3. XPS analysis

Fig. 3 shows the XPS depth profile of the passive film prepared by tungstate/nitric and tungstate/phosphoric solutions. Both passive films were mainly composed of zinc and oxygen species, in which the
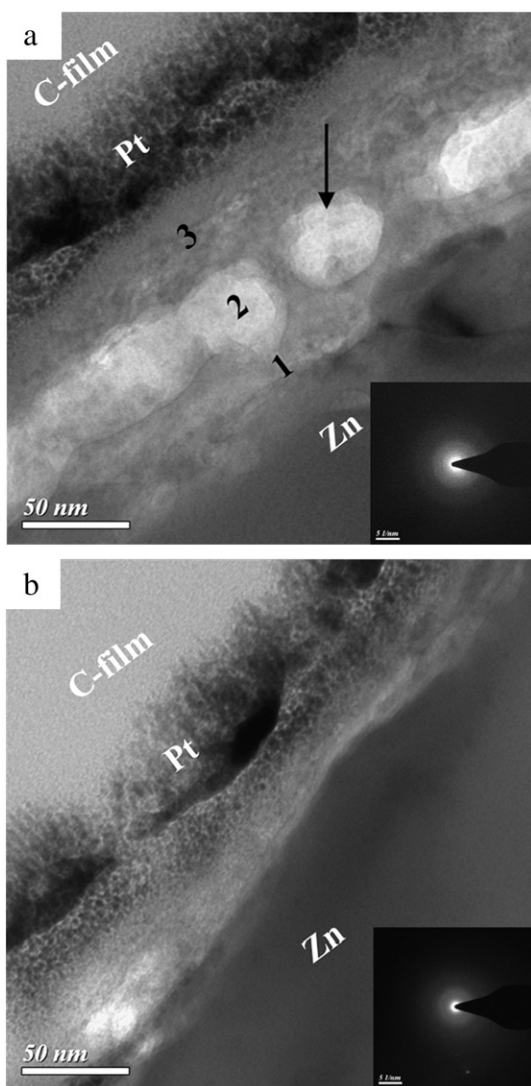

Fig. 2. Cross-sectional TEM micrographs of the passive film prepared by (a) tungstate/nitric and (b) tungstate/phosphoric solutions. The Pt layer and C-film are deposited prior to the preparation of TEM samples via FIB.
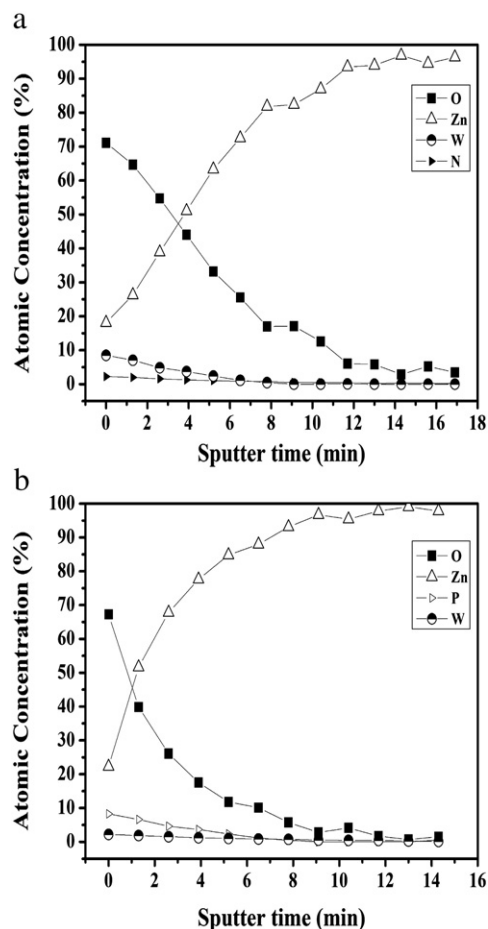

Fig. 3. XPS depth profile of the passive film prepared by (a) tungstate/nitric and (b) tungstate/phosphoric solutions.

zinc content increased and the oxygen content decreased along the depth of the passive film. In contrast, the tungsten, nitrogen, and phosphorus contents exhibited a monotonous decrease along the depth of the passive film. Furthermore, the passive film prepared by the tungstate/nitric solution contained more tungsten species than that prepared by the tungstate/phosphoric solution. Fig. 4 shows a high-resolution spectrum of tungsten W 4f, in which two peaks corresponded to metallic tungsten, W, and tungsten dioxide, WO_2, and two peaks were associated with tungstate ion, WO_4^{2-} and tungsten trioxide, WO_3[24–29].Fig. 4 also shows that the ratio of metallic W and WO_2 to the total tungsten species in the passive film prepared by the tungstate/nitric solution was larger than that of the passive film prepared by the tungstate/phosphoric solution.

3.4. Polarization measurements

Fig. 5 shows the polarization curves of the GI steels without and with the tungstate passivation treatment. Compared with the GI steel without passivation treatment, the polarization curves of the GI steels with the tungstate passivation treatment shifted towards lower current densities and nobler potentials, suggesting the tungstate
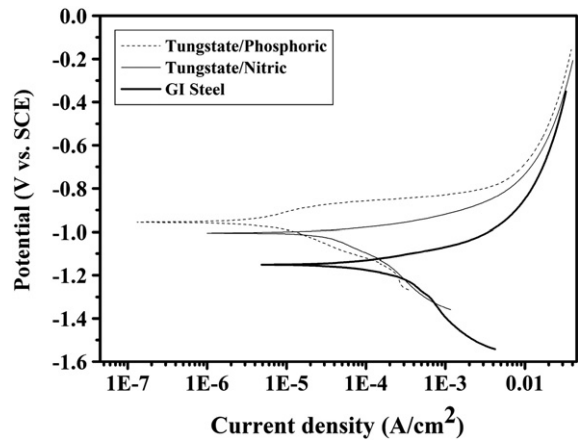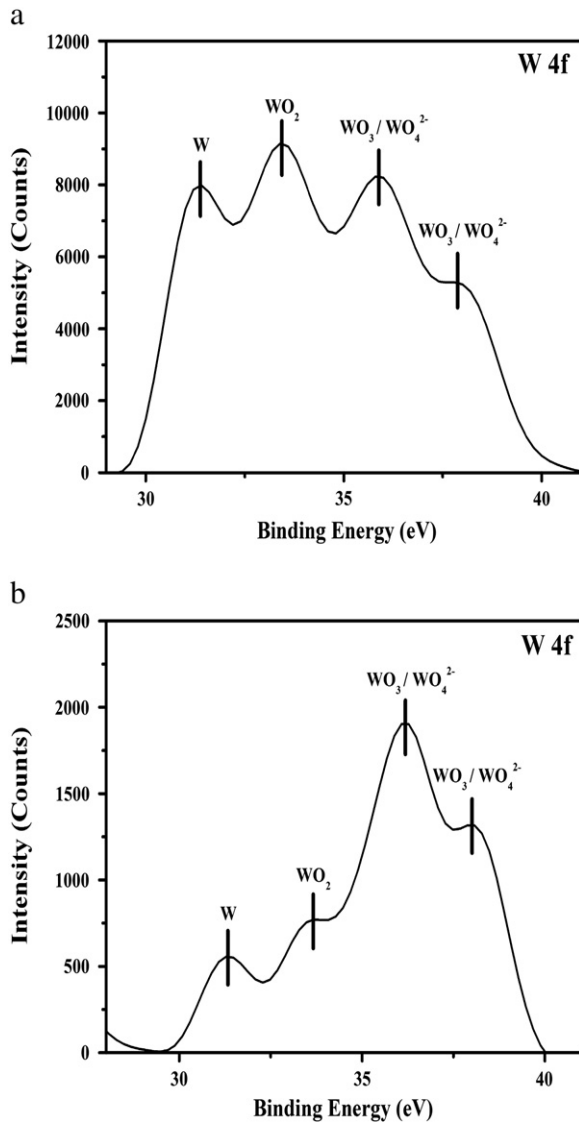

Fig. 4. W 4f XPS spectra of the passive film prepared by (a) tungstate/nitric and (b) tungstate/phosphoric solutions.

Fig. 5. Polarization curves of the various GI samples in 5 wt.% NaCl.

passivation treatment improved the corrosion resistance of the GI steel. The corrosion potential (E_{corr}) and corrosion current density (I_{corr}) measured from extrapolation of the Tafel region of the cathodic branch to the E_{corr} are summarized in Table 2. The GI steel treated with the tungstate/phosphoric solution had a nobler corrosion potential and a lower corrosion current density than that treated with the tungstate/nitric solution. Moreover, the tungstate/phosphoric passive film had significantly lower anodic current density than that of the tungstate/nitric passive film. Consequently, the tungstate/phosphoric passive film has better corrosion resistance than that of the tungstate/nitric passive film.

4. Discussion

4.1. Formation of the passive film during roll coating process

It has been generally recognized that the formation of conversion coating relies on the increase in surface pH resulting from hydrogen evolution accompanying the oxidation and dissolution of the substrate [14,18]. The tungstate solution for the roll coating process investigated in this study has a pH value of 2.5. Once covered with a pH 2.5 liquid film applied via roll coating, the zinc layer of the GI steel dissolves immediately, together with the reduction of hydrogen ions. Hydrogen discharge causes an increase in pH value at the interface between the zinc substrate and the solution. The high-pH environment favors the precipitation of zinc hydroxide and zinc phosphate. From the XPS and TEM/EDS results, the passive film prepared by the tungstate/nitric solution is composed of zinc oxide/hydroxide as the major constituent , with traces of metallic W, tungsten species of various valences (WO_2, WO_3, WO_4^{2-}), and nitrogen species.

The tungstate solution studied contains 0.08 M WO_4^{2-}, which is colorless and stable at a pH greater than 6.5 according to the Pourbaix diagram of tungsten–water system. In the 0.08 M tungstate solution, WO_4^{2-} precipitates to form yellow WO_3 (Reaction 1) as the pH of the solution is below 6.5 [30].

$$WO_4^{2-} + 2H^+ \rightarrow WO_3 + H_2O \tag{1}$$

Table 2
E_{corr} and I_{corr} of the various GI samples in 5 wt.% NaCl.

Specimen	E_{corr} (V vs. SCE)	I_{corr} ($\mu A/cm^2$)
GI steel	−1.151	78.672
Tungstate/nitric	−1.004	28.821
Tungstate/phosphoric	−0.955	4.422

However, yellow WO_3 precipitates were not observed in the 0.08 M tungstate solution with pH 2.5 by naked eyes and optical microscopy after two months. This suggests that speciation and equilibrium of WO_3 from WO_4^{2-} can be very slow and the major form of tungsten species in the tungstate/phosphoric and tungstate/nitric solutions at pH 2.5 is WO_4^{2-}. The presence of WO_3 in the passive film may result from water evaporation during the baking step of the roll coating process, which promotes Reaction (1) toward the right-hand side reaction.
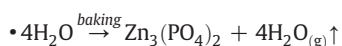
After the water in the liquid film evaporated completely, WO_4^{2-}, NO_3^-, HPO_4^{2-}, and PO_4^{3-} anions are absorbed into the passive film. The presence of WO_2 and metallic W suggests that WO_4^{2-} can be reduced to WO_2 and metallic W in accompany with the oxidation of zinc in both tungstate/nitric and tungstate/phosphoric solutions, as shown by Reactions 2 and 3.

$$WO_4^{2-} + 4H^+ + 2e^- \rightarrow WO_2 + 2H_2O \qquad (2)$$

$$WO_4^{2-} + 8H^+ + 6e^- \rightarrow W + 4H_2O \qquad (3)$$
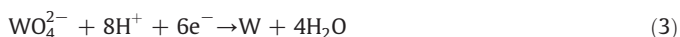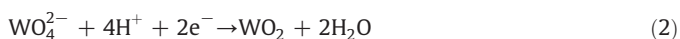
Cross-sectional TEM observations revealed that the passive film prepared by the tungstate/nitric solution is thicker and more porous than that prepared by the tungstate/phosphoric solution. Similar results have been found in molybdate/nitric and molybdate/phosphoric conversion coatings on 99.9 pure zinc and electrogalvanized steel prepared via an immersion coating process [13]. The nitrate anion in the tungstate solution act as an accelerator (Reaction (4)) [2], which tends to enhance the oxidation of zinc, together with the reduction of WO_4^{2-} to WO_2 and metallic W, as well as hydrogen evolution. The spherical voids observed in the passive film prepared by the tungstate/nitric solution can result from the incorporation of hydrogen bubbles whose formation is promoted in the presence of nitrate anions.

$$NO_3^- + 2H^+ + 2e^- \rightarrow NO_2^- + H_2O \qquad (4)$$
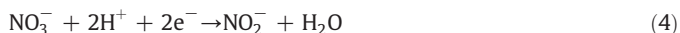
In the tungstate/phosphoric solution, the dissolution of zinc results in an increase in interfacial pH, meanwhile dihydrogen phosphate anions dissociate to hydrogen phosphate and phosphate anions with increasing pH. As a result, Zn^{2+} dissolved from the Zn substrate react with phosphate and hydroxyl anions to cause the precipitation of zinc hydroxide ($K_{sp} = 3 \times 10^{-17}$) and zinc phosphate ($K_{sp} = 5 \times 10^{-36}$) [31]. Phosphoric acid in the tungstate/phosphoric solution provides PO_4^{3-} to form zinc phosphate (Reaction (5)). However, they have little effect on promoting the oxidation of zinc and the accompanying reduction of WO_4^{2-} anions. As a result, less metallic tungsten and WO_2 were incorporated in the passive film prepared by the tungstate/phosphoric solution.

$$3Zn^{2+} + 2PO_4^{3-} + 4H_2O \rightarrow Zn_3(PO_4)_2 \qquad (5)$$

$$\cdot 4H_2O \overset{baking}{\rightarrow} Zn_3(PO_4)_2 + 4H_2O_{(g)} \uparrow$$

Although the above-mentioned reactions occur upon applying a tungstate liquid film and during the subsequent baking at 200 °C, the change in the surface morphology of the GI steel is slight, and the specimens treated with tungstate/nitric and tungstate/phosphoric solutions exhibit an insignificant difference in the surface morphology. This is due to the fact that the conversion coating is very thin, i.e. less than 100 nm, as characterized by cross-sectional TEM (Fig. 2). Moreover, the tungstate conversion coatings prepared by roll coating are free of cracks, which were commonly seen in the conversion coatings prepared by immersion. Da Silva et al. [18] studied the effect of the solution pH and tungstate concentration on the corrosion resistance and microstructure of the tungstate conversed Zn and electrogalvanized steels, as well as the surface pH and OCP evolution during the conversion

coating treatment. They found that the tungstate solution acidified with phosphoric acid afforded the substrate the best corrosion resistance and in the pH ranging from 1 to 7, the conversion coating with optimal corrosion resistance can be made after 1 min of immersion in the pH 3 solution. Furthermore, the surface morphology of the coating markedly depended on the solution pH. After 1 min of immersion, the conversion coating formed at pH 1 displayed a rough morphology, while that formed at pH 3 had a relatively smooth surface. However, the coating formed after prolonged immersion (20 min) in pH 3 solution contained cracks. The presence of cracks is due to the stress associated with volume shrinkage during the drying step. Further increasing the solution pH to 5 and 7 deteriorated the corrosion resistance although
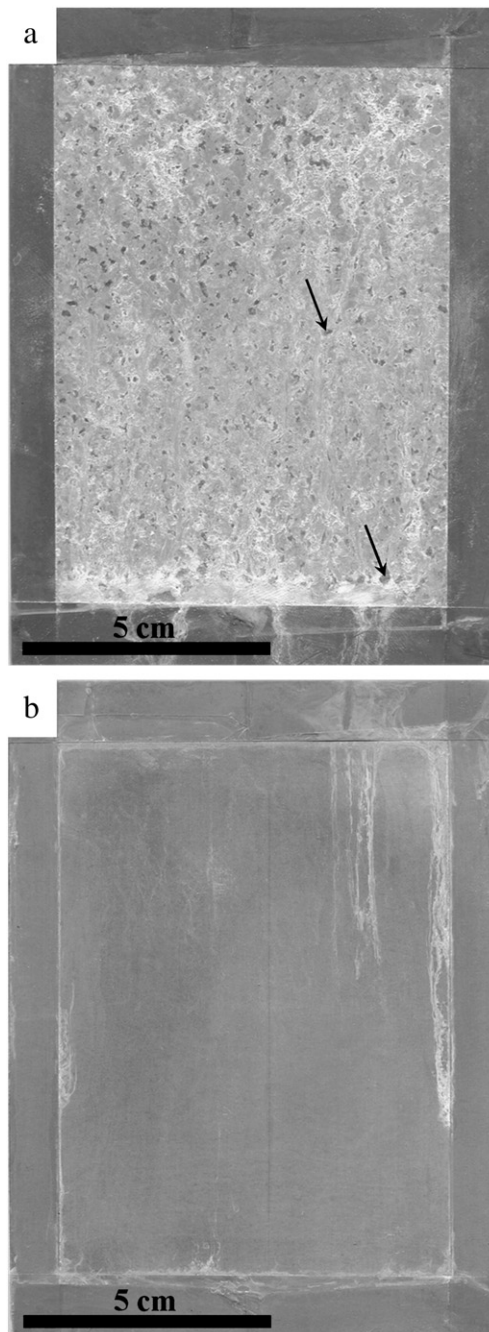

Fig. 6. The pictures of the (a) tungstate/nitric and (b) tungstate/phosphoric passivated GI steels after 24 h of neutral salt spray test.

the hydrogen evolution reaction was less intense and the conversion coating developed faster at higher pH.

4.2. Corrosion resistance mechanism of the passive coating on GI steel via roll coating process

The results of polarization curves show that the GI steel treated with the tungstate/phosphoric solution has better corrosion resistance than that treated with the tungstate/nitric solution. The neutral salt spray test with 5 wt.% NaCl was further employed to evaluate the corrosion resistance of the various samples. Fig. 6a shows the picture of the tungstate/nitric passivated GI steel after 24 h of salt spray test. The surface appeared in both the white areas and the dark areas (indicated by the arrow). The white areas were associated with the zinc corrosion products (white rust). However, magnified observation using an optical microscope revealed that the dark areas appeared in a shiny morphology (not shown here), which is similar to that of the as-received GI steel. As a result, the white areas and dark areas represent the Zn coating after corrosion and that free of corrosion, respectively. Unlike the severe corrosion of the tungstate/nitric passivated GI steel, the white rust area of the tungstate/phosphoric passivated GI steel was less than 5% after 24 h of salt spray test (Fig. 6b). The better corrosion resistance afforded by the tungstate/phosphoric conversion coating than the tungstate/nitric counterpart agrees well with the results made by Magalhaes et al. who found that the molybdate solution acidified with phosphoric acid resulted in the molybdate conversion coating with best corrosion resistance [13].

Consequently, the performance of the tungstate passive film on GI steel strongly depends on the composition of the passivation solutions. The passive film prepared by the tungstate/phosphoric solution is more compact than that prepared by the tungstate/nitric solution, as shown in the cross-sectional TEM micrographs (Fig. 2). Furthermore, zinc phosphate has better corrosion resistance than zinc hydroxide in neutral salt solution. Metallic tungsten is also less corrosion-resistant than tungsten oxides in neutral salt solution. Therefore, compared with that prepared by the tungstate/nitric solution, less metallic tungsten in the passive film prepared by the tungstate/phosphoric solution further improves the corrosion resistance of the passive film. Finally, the higher ratio of hexavalent tungsten (WO_3 and WO_4^{2-}) to the total tungsten species for the passive film prepared by the tungstate/phosphoric solution (Fig. 4) further contributes to the enhanced corrosion resistance compared to that prepared by the tungstate/nitric solution. The presence of WO_4^{2-} in the passive film also plays an inhibition role in preventing the passive film from corrosion attack. During corrosion attack, WO_4^{2-} anions are liberated from the passive film, adsorbed on the exposed zinc surface, which, in turn, leads to the formation of a layer impermeable to other anions such as Cl^-. Moreover, the reduced forms of WO_4^{2-} anions can be incorporated in the corrosion products and repair the flawed regions of the passive film, which effectively reduces the pitting susceptibility [19–21].

5. Conclusions

A passive film was applied onto GI steel using a roll coating process with tungstate/phosphoric or tungstate/nitric solutions. Several conclusions have been reached based on the microstructure and corrosion resistance of the passive film.

1. The surface morphology of GI steel slightly changed after the roll coating treatment in both the tungstate/nitric and tungstate/phosphoric solutions. Moreover, insignificant difference in the surface morphology was observed for the GI steels treated with the tungstate/nitric and tungstate/phosphoric solutions.

2. Cross-sectional TEM characterization revealed that the tungstate/nitric passive film was thicker and more porous than the tungstate/phosphoric passive film, as evident by the presence of relatively-large voids in the tungstate/nitric passive film.

3. In addition to zinc oxide/hydroxide, low-valent tungsten oxide, metallic tungsten and remnants of the various anions were also detected in the tungstate passive film.

4. The GI steel treated with the tungstate/phosphoric solution displayed a better corrosion resistance than that treated with the tungstate/nitric solution. The better performance of the passive film prepared by the tungstate/phosphoric solution can be attributed to the presence of zinc phosphate in the relatively compact passive film. Moreover, less metallic tungsten and more hexavalent tungsten species in the passive film further improved the corrosion resistance of the passive film prepared by the tungstate/phosphoric solution.

Acknowledgement

References

[1] M. Wolpers, J. Angeli, Appl. Surf. Sci. 179 (2001) 281.
[2] D. Zimmermann, A.G. Munoz, J.W. Schultze, Surf. Coat. Technol. 197 (2005) 260.
[3] K. Ogle, A. Tomandl, N. Meddahi, M. Wolpers, Corros. Sci. 46 (2004) 979.
[4] A.S. Akhtar, D. Susac, P. Glaze, K.C. Wong, P.C. Wong, K.A.R. Mitchell, Surf. Coat. Technol. 187 (2004) 208.
[5] S. Jegannathan, T.S.N. Sankara Narayanan, K. Ravichandran, S. Rajeswari, Surf. Coat. Technol. 200 (2006) 4117.
[6] B.L. Lin, J.T. Lu, G. Kong, Corros. Sci. 50 (2008) 962.
[7] B.L. Lin, J.T. Lu, G. Kong, Surf. Coat. Technol. 202 (2008) 1831.
[8] K. Aramaki, Corros. Sci. 43 (2001) 2201.
[9] M.F. Montemor, A.M. Simoes, M.G.S. Ferreira, Prog. in Org. Coat. 43 (2001) 274.
[10] D.E. Walkers, G.D. Wilcox, Trans. Inst. Met. Fin. 86 (2008) 251.
[11] G.M. Treacy, G.D. Wilcox, M.O.W. Richardson, J. Appl. Electrochem. 29 (1999) 647.
[12] H. Konno, K. Narumi, H. Habazaki, Corros. Sci. 44 (2002) 1889.
[13] A.A.O. Magalhaes, I.C.P. Margarit, O.R. Mattos, J. Electroanal. Chem. 572 (2004) 433.
[14] C.G. da Silva, I.C.P. Margarit-Mattos, O.R. Mattos, H. Perrot, B. Tribollet, V. Vivier, Corros. Sci. 51 (2009) 151.
[15] Y.K. Song, F. Mansfeld, Corros. Sci. 48 (2006) 154.
[16] E. Almeida, T.C. Diamantino, M.O. Figueiredo, C. Sa, Surf. Coat. Technol. 106 (1998) 8.
[17] R.E. Van De Leest, G. Krijl, Thin Solid Films 72 (1980) 237.
[18] C.G. da Silva, A.N. Correia, P. de Lima-Neto, I.C.P. Margarit, O.R. Mattos, Corros. Sci. 47 (2005) 709.
[19] M.A. Amin, Electrochim. Acta 50 (2005) 1265.
[20] M.A. Amin, H.H. Hassan, S.S.A.E. Rehim, Electrochim. Acta 53 (2008) 2600.
[21] E.E. Abd El Aal, S. Abd El Wanees, Corros. Sci. 51 (2009) 1780.
[22] E. Szczurek, M. Dubar, R. Deltombe, A. Dubois, L. Dubar, J. Mater. Proce. Tech. 209 (2009) 3187.
[23] N.T. Wen, F.J. Chen, M.D. Ger, Y.N. Pan, C.S. Lin, Electrochem. Solid –State Lett. 11 (2008) C47.
[24] J.F. Moulder, W.F. Stickle, P.E. Sobol, K.D. Bomben, Handbook of X-ray Photoelectron Spectroscopy, Physical Electronics Inc., Minnesota, USA, 1992.
[25] A. Pakes, P. Skeldon, G.E. Thompson, S. Moisa, G.I. Sproule, M.J. Graham, Corros. Sci. 44 (2002) 2161.
[26] P. Charton, L. Gengembre, P. Armand, J. Solid State Chem. 168 (2002) 175.
[27] A. Suleiman, P. Skeldon, G.E. Thompson, F. Echeverria, M.J. Graham, G.I. Sproule, S. Moisa, T. Quance, H. Habazaki, Corros. Sci. 52 (2010) 595.
[28] X.G. Wang, Y.S. Jang, N.H. Yang, L. Yuan, S.J. Pang, Surf. Coat. Technol. 99 (1998) 82.
[29] A.K.L. Sajjad, S. Shamaila, B. Tian, F. Chen, J. Zhang, Appl. Catalysis B: Environ. 91 (2009) 397.
[30] M. Pourbaix, Atlas of Electrochemical Equilibria in Aqueous Solutions, National Association of Corrosion Engineers, Houston, Texas, USA, 1974.
[31] D.R. Lide, Handbook of Chemistry and Physics, 88th ed CRC Press, Florida, USA, 2007–2008.